Cluster model of ^{12}C in the density functional theory framework

A. S. Umar [1,*] K. Godbey [2,†] and C. Simenel [3,‡]

[1]*Department of Physics and Astronomy, Vanderbilt University, Nashville, Tennessee 37235, USA*

[2]*Facility for Rare Isotope Beams, Michigan State University, East Lansing, Michigan 48824, USA*

[3]*Department of Fundamental and Theoretical Physics and Department of Nuclear Physics and Accelerator Applications, Research School of Physics, The Australian National University, Canberra ACT 2601, Australia*

(Received 23 April 2023; accepted 19 May 2023; published 14 June 2023)

We employ the constrained density functional theory to investigate cluster phenomena for the ^{12}C nucleus. The proton and neutron densities are generated from the placement of three ^{4}He nuclei (α particles) geometrically. These densities are then used in a density constrained Hartree-Fock calculation that produces an antisymmetrized state with the same densities through energy minimization. In the calculations no *a priori* analytic form for the single-particle states is assumed and the full energy density functional is utilized. The geometrical scan of the energy landscape provides the ground state of ^{12}C as an equilateral triangular configuration of three αs with molecular bond like structures. The use of the nucleon localization function provides further insight to these configurations. One can conclude that these configurations are a hybrid between a pure mean-field and a pure α particle condensate. This development could facilitate density functional theory based fusion calculations with a more realistic ^{12}C ground state.

DOI: 10.1103/PhysRevC.107.064605

I. INTRODUCTION

In stellar evolution carbon plays a pivotal role through the carbon burning process. The ignition of carbon burning for stars in the mass range $M > 8$–10 solar masses lead to white Ne/O dwarfs, while massive stars with masses $M > 25$ solar masses can continue burning Ne, O, and Si and end up as supernovae. Similarly, Type Ia supernovae are believed to result from an explosion of a white dwarf accreting mass from a binary companion or a merger, inducing high enough temperatures to ignite carbon in the core leading to a supernovae explosion. Superbursts are set off by the ignition of carbon in the accumulated ashes of previous x-ray bursts [1–3]. Overall, a change in the ^{12}C $+^{12}$C reaction rates has a profound impact on all these mechanisms as well as nucleosynthesis [4–11]. In the stellar environment carbon is produced in a two step process; in the first step two ^{4}He nuclei come together to form an unstable ^{8}Be, which decays back to two ^{4}He nuclei with a very short lifetime (10^{-16}s). However, during the helium burning stage, the densities are high enough to maintain a small abundance of ^{8}Be, which renders it possible to combine with another ^{4}He to form an excited carbon nucleus through the well known Hoyle state of ^{12}C. With a much lower probability a triple ^{4}He combination may also lead to the same outcome.

In addition to its astrophysical importance, the microscopic description of the carbon nucleus, which is an essential ingredient to the reaction calculations, has proven to be a challenge. This is predicated by the expectation that the structure of carbon should exhibit a pronounced cluster structure. Clustering effects are widely believed to play prominent role in the structure of $N = Z$ nuclei, resulting in a molecular type phenomenon. To what degree such nuclei can be viewed as being comprised of a pure α particle condensate is still an open question [12].

However, employing the standard nonrelativistic density functional theory (DFT) results in a ground state of ^{12}C without any sign of clusterization [13]. This is also true for ^{16}O, while the ground states of ^{8}Be and ^{20}Ne do show some cluster features [13]. Relativistic mean-field theories seem to favor more clusterization due to deeper potentials [14]. Alternate approaches of using configuration mixing with generator coordinate method (GCM) calculations using the Skyrme energy density functional have also been done in Refs. [15,16]. Furthermore, these calculations using modern energy density functionals commonly result in a spherical ground state for the ^{12}C nucleus, which is experimentally known to have an oblate deformation [17–19]. On the other hand the excited states of these nuclei do seem to exhibit some cluster structure, e.g., the linear-chain configuration of ^{12}C, which originally was thought to be the Hoyle state [20], and excited states obtained by various constraints [14,21–30]. Such formations are also observed via the time-dependent Hartree-Fock studies of the triple-α reaction [31,32] and studied in recent experiments [33,34]. In these time-dependent calculations a bent-arm intermediate configuration is observed during the decay of the metastable linear chain state of ^{12}C.

The fact that DFT calculations account for only limited clustering effects prompted alternate approaches to study ^{12}C

*umar@compsci.cas.vanderbilt.edu

†godbey@frib.msu.edu

‡cedric.simenel@anu.edu.au

structure that rely more heavily on cluster wave functions. These calculations suggest that a substantial contribution of alpha cluster correlations that are not accounted for in the mean-field description should nevertheless be present in ^{12}C states. These include various *ab initio* calculations [35–37] as well as approaches that are collectively referred to as molecular dynamics that significantly extend the original Bloch-Brink α cluster model [38]. In Brink's approach each quartet of nucleons where represented using harmonic oscillator wave functions with zero angular momentum displaced from each other by a relative coordinate. Antisymmetrization followed by normalization comprised the many-body wave function in terms of the locations of the quartets. These quartets, interacting via an effective nucleon-nucleon interaction, are optimized with respect to their size and position to map out the energy landscape showing the location of the minima. This approach was extended via the resonating group method as well as generator coordinate method to better incorporate the internal structure of the clusters. The antisymmetrized molecular dynamics (AMD) [39–41] approach employs a Slater determinental many-body wave function comprised of single-particle states as Gaussian wave packets using an advanced set of geometrical variables. Fermionic molecular dynamics (FMD) [42] further extends AMD by not putting any restriction on the width of these Gaussians. These calculations indicate a large admixture of α-cluster triangular states for the ground and some of the excited states configurations of ^{12}C. The use of Gaussian basis and suitable interactions allow for very powerful extensions for the above methods, such as the treatment of the center-of-mass energy, angular momentum projection, and the use of the generator coordinate method (GCM). However, many of these calculations assume a degeneracy between neutron and proton wave functions and do not include the full effective interaction and the spin-orbit force. A collection of recent reviews can be found in Refs. [12,43–47].

In this paper we introduce another approach for studying cluster structures within the DFT framework. This is accomplished through the use of the density constrained Hartree-Fock approach. Here, we start with α particles as solutions to the unconstrained Hartree-Fock (HF) equations. These α particles are then geometrically arranged on the numerical grid defining the total density of the system. For each arrangement, a mean-field solution is obtained through minimization of the energy by constraining the density of the entire system. Density constraint iterations allow for the rearrangement of the single-particle states through their orthogonalization and energy minimization. This takes care of antisymmetrization as well as the overall energy dependent normalization of the many-body wave function. No assumption about the mathematical form of the single-particle states is made and the full effective interaction, including the Coulomb force, can be used. We also employ the nuclear localization function (NLF), which allows for a more precise characterization of spatial distributions. This method blends the cluster based approach with the fully microscopic approach. As we shall see, it has advantages and certain disadvantages.

II. MICROSCOPIC METHODS

In this section we briefly outline the formalisms and methods used in our calculations. Further details can be found in the cited references.

A. Density constraint

Given a reference density, the density constraint procedure [48,49] allows the single-particle states, comprising the combined nuclear density, to reorganize to attain their minimum energy configuration and be properly antisymmetrized as the many-body state is a Slater determinant of all the occupied single-particle wave functions. Here, the reference density is given by the combined density of three α particles obtained from independent Hartree-Fock calculations and placed in close proximity of each other. The HF minimization of the combined system is thus performed subject to the constraint that the local proton (p) and neutron (n) densities do not change:

$$\delta\left\langle H - \sum_{q=p,n}\int d\mathbf{r}\,\lambda_q(\mathbf{r})\left[\sum_{i=1}^{3}\rho_{i_q}^{\alpha}(\mathbf{r},\mathbf{R_i})\right]\right\rangle = 0\,, \qquad (1)$$

where the $\lambda_{n,p}(\mathbf{r})$ are Lagrange parameters at each point of space constraining the neutron and proton local densities, $\rho_{i_q}^{\alpha}(\mathbf{r},\mathbf{R_i})$ is the proton/neutron densities of an α particle located at position $\mathbf{R_i}$, and H is the effective many-body Hamiltonian. This procedure determines a unique Slater determinant $|\Phi(\mathbf{R_1},\mathbf{R_2},\mathbf{R_3})\rangle$ for the combined system. The density constraint has been extensively used in the calculation of ion-ion interaction barriers for fusion calculations [50–52].

B. Center of mass correction

A major drawback of any mean-field based microscopic calculation is the uncontrolled presence of the energy associated with the center-of-mass (c.m.) motion [53]. This energy is particularly large for light nuclei. Most Skyrme interactions adopt a simple one-body correction for this energy, which may be reasonable for heavy systems. This issue has been discussed more extensively in the context of α clustering phenomenon for the mean-field calculations in Ref. [23], where a constant value of 7 MeV per α particle was subtracted. However, the c.m. correction for a composite system may not be the same as adding corrections for each α. Due to this we cannot make any binding energy comparisons and adopted the SLy4d interaction, which does not employ any center-of-mass correction term.

C. The nucleon localization function (NLF)

The measure of localization has been originally developed in the context of a mean-field description for electronic systems [54], and subsequently introduced to nuclear systems [13,55,56]. We first realize that a fermionic mean-field state is fully characterized by the one-body density-matrix $\rho_q(\mathbf{r}s,\mathbf{r}'s')$. The probability of finding two nucleons with the same spin at spatial locations $\mathbf{r}$ and $\mathbf{r}'$ (same-spin pair

probability) for isospin q is proportional to

$$P_{qs}(\mathbf{r},\mathbf{r}') = \rho_q(\mathbf{r}s,\mathbf{r}s)\rho_q(\mathbf{r}'s,\mathbf{r}'s) - |\rho_q(\mathbf{r}s,\mathbf{r}'s)|^2\,, \quad (2)$$

which vanishes for $\mathbf{r}=\mathbf{r}'$ due to the Pauli exclusion principle. The conditional probability for finding a nucleon at $\mathbf{r}'$ when we know with certainty that another nucleon with the same spin and isospin is at $\mathbf{r}$ is proportional to

$$R_{qs}(\mathbf{r},\mathbf{r}') = \frac{P_{qs}(\mathbf{r},\mathbf{r}')}{\rho_q(\mathbf{r}s,\mathbf{r}s)}\,. \quad (3)$$

The short-range behavior of R_{qs} can be obtained using techniques similar to the local density approximation [13,55]. The leading term in the expansion yields the localization measure

$$D_{qs_\mu} = \tau_{qs_\mu} - \frac{1}{4}\frac{|\nabla\rho_{qs_\mu}|^2}{\rho_{qs_\mu}} - \frac{|\mathbf{j}_{qs_\mu}|^2}{\rho_{qs_\mu}}\,. \quad (4)$$

This measure is the most general form that is appropriate for deformed nuclei and without assuming time-reversal invariance, thus also including the time-odd terms important in applications such as cranking or time-dependent Hartree-Fock (TDHF). The densities and currents are given in their most unrestricted form [57–59] for μ axis denoting the spin-quantization axis by [55]

$$\rho_{qs_\mu}(\mathbf{r}) = \tfrac{1}{2}\rho_q(\mathbf{r}) + \tfrac{1}{2}\sigma_\mu s_{q\mu}(\mathbf{r})\,, \quad (5a)$$

$$\tau_{qs_\mu}(\mathbf{r}) = \tfrac{1}{2}\tau_q(\mathbf{r}) + \tfrac{1}{2}\sigma_\mu T_{q\mu}(\mathbf{r})\,, \quad (5b)$$

$$\mathbf{j}_{qs_\mu}(\mathbf{r}) = \tfrac{1}{2}\mathbf{j}_q(\mathbf{r}) + \tfrac{1}{2}\sigma_\mu \mathbb{J}_q(\mathbf{r})\cdot\mathbf{e}_\mu\,, \quad (5c)$$

where $\sigma_\mu = 2s_\mu = \pm 1$ and $\mathbf{e}_\mu$ is the unit vector in the direction of the μ axis. Note that subscripts s_μ denote spin along the quantization axis and should not be confused by the spin-density $s_{q\mu}$. The dot product in Eq. 5(c) is explicitly given in the case of, e.g., $\mu = z$,

$$\mathbb{J}_q(\mathbf{r})\cdot\mathbf{e}_z = \frac{1}{2i}[(\nabla-\nabla')s_{qz}(\mathbf{r},\mathbf{r}')]_{\mathbf{r}=\mathbf{r}'}\,.$$

The explicit expressions of the local densities and currents are given in Refs. [55,57]. We note that the localization measure includes the spin-density $s_{q\mu}(\mathbf{r})$, the time-odd part of the kinetic density $T_{q\mu}(\mathbf{r})$, as well as the full spin-orbit tensor $\mathbb{J}_q(\mathbf{r})$, which is a pseudotensor. In this sense all of the terms in the Skyrme energy density functional [57] contribute to the measure. Finally, we note that the time-odd terms contained in the above definitions ($s_{q\mu}$, $T_{q\mu}$, and $\mathbf{j}_q$) are zero in static calculations of even-even nuclei but the spin-tensor $\mathbb{J}_q$ is not. Therefore, $\mathbf{j}_{qs_\mu}$ is not zero in general.

It is interesting to visualize the NLF as it is also defined from the localization measure in Eq. (4). We first normalize the localization measure using [55]

$$\mathcal{D}_{qs_\mu}(\mathbf{r}) = \frac{D_{qs_\mu}(\mathbf{r})}{\tau^{\rm TF}_{qs_\mu}(\mathbf{r})}\,, \quad (6)$$

where the normalization $\tau^{\rm TF}_{qs_\mu}(\mathbf{r}) = \frac{3}{5}(6\pi^2)^{2/3}\rho^{5/3}_{qs_\mu}(\mathbf{r})$ is the Thomas-Fermi kinetic density. The NLF can then be represented either by $1/\mathcal{D}_{qs_\mu}$ or by

$$C_{qs_\mu}(\mathbf{r}) = \left[1+\mathcal{D}^2_{qs_\mu}\right]^{-1} \quad (7)$$

which is used here. The advantage of the latter form is that it scales to be in the interval [0,1], but otherwise both forms show similar localization details.

The information content of the localization function is better understood by considering limiting cases. The extreme case of ideal metallic bonding is realized for homogeneous matter where $\tau = \tau^{\rm TF}_{q\sigma}$. This yields $C = \frac{1}{2}$, a value which thus signals a region with a nearly homogeneous Fermi gas as it is typical for metal electrons, nuclear matter, or neutron stars. The opposite regime are space regions where exactly one single-particle wave function of type $q\sigma$ contributes. This is called *localization* in molecular physics. Such a situation yields $D_{q\sigma}(\mathbf{r}) = 0$, since it is not possible to find another like-spin state in the vicinity, and consequently $C = 1$, the value which signals *localization*.

In the nuclear case, it is the α particle which is perfectly localized in this sense, i.e., which has $C = 1$ everywhere for all states. Well bound nuclei show usually metallic bonding and predominantly have $C = \frac{1}{2}$. Light nuclei are often expected to contain pronounced α-particle substructures. Such a substructure means that in a certain region of space only an α particle is found which in turn is signaled by $C = 1$ in this region. In fact, an α substructure is a correlation of four particles: $p\uparrow$, $p\downarrow$, $n\uparrow$, and $n\downarrow$. Thus it is signaled only if we find simultaneously for all four corresponding localization functions $C_{q\sigma} \approx 1$. This localization procedure was recently employed to visualize the cluster structure in $N = Z$ light nuclei [60].

D. Numerical details

Calculations were done in a three-dimensional Cartesian geometry with no symmetry assumptions using the code of Ref. [61] and using the Skyrme SLy4d interaction [62], which has been successful in describing various types of nuclear reactions [50,63]. The three-dimensional Poisson equation for the Coulomb potential is solved by using fast-Fourier transform techniques and the Slater approximation is used for the Coulomb exchange term. The static HF equations and the density constraint minimizations are implemented using the damped gradient iteration method [64]. The box size used for all the calculations was chosen to be $24\times24\times24$ fm^3 with a mesh spacing of 1.0 fm in all directions. These values provide very accurate results due to the employment of sophisticated discretization techniques [65,66].

III. RESULTS

The placement of the three α particles were done as follows: Two α particles were placed on the x axis with a spacing denoted by $d_2/2$ on each side of the origin. The third α particle was placed at distance z_3 vertically from the origin. There are numerous studies of α cluster models for ^{12}C that show that this more symmetric arrangement leads to the minimum energy configuration [46], as anticipated from symmetry arguments. Moving the third α in the y direction would simply correspond to tilting the three-α system in the three-dimensional (3D) space. We have scanned d_2 values

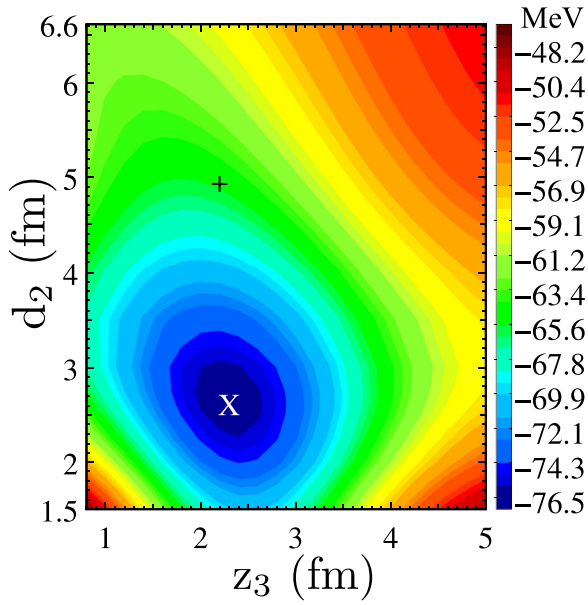

FIG. 1. The 3-α energy surface obtained from the density constraint procedure as a function of the spacings d_2 and z_3. The point marked by X indicates the location of the minimum.

ranging from 1.5–6.6 fm in steps of 0.1 fm. For each value of d_2, z_3 was varied from 0.7–5.0 fm in steps of 0.2 fm. When necessary we have used a smaller spacing to pinpoint the desired location more precisely. For $z_3 < 0.7$ the large overlap among the three αs lead to convergence problems due to unphysically large densities.

In Fig. 1 we plot the 3-α energy surface as a function of the spacings d_2 and z_3 obtained by the density constrained minimization procedure. The minimum energy is obtained for $d_2 = 2.65$ fm and $z_3 = 2.3$ fm. This numerically obtained minimum corresponds to an equilateral triangle placement of α particles, and is identified as the ground state. These findings are in agreement with other cluster model calculations (see for example [46]). In Fig. 2(a) we plot the ground state density as well as the localization function for the ground state of ^{12}C in the x-z plane. The density has a triangular shape and looks relatively compact with an octupole deformation. Experimentally deduced mass radius of ^{12}C is 2.43 fm [67,68]. Different cluster model calculations yield a range of 2.40–2.53 fm [40]. Our calculations result in a slightly larger radius of 2.57 fm. The quadrupole deformation for ^{12}C is experimentally deduced to be oblate with $\beta_2 = -0.4$ [17,69]. Cluster calculations of Ref. [29] found $\beta_2 = -0.41$ and $\gamma = 27.5^\circ$. Our calculations find $\beta_2 = -0.42$ and $\gamma = 29.7^\circ$.

Figure 2(b) shows the $n\uparrow$ localization function immediately after placing the three αs in their appropriate locations but before the start of the density constraint iterations. As we have mentioned above, for a single α particle the localization has a fixed value of 1.0 throughout. Thus the mere combination of three αs does show a significant localization. However, the dominant localization is still 1.0 suggesting a pure α makeup. The density constraint minimization modifies this localization function as shown in Fig. 2(c). The α substructure of the ground state is still clearly pronounced. The regions

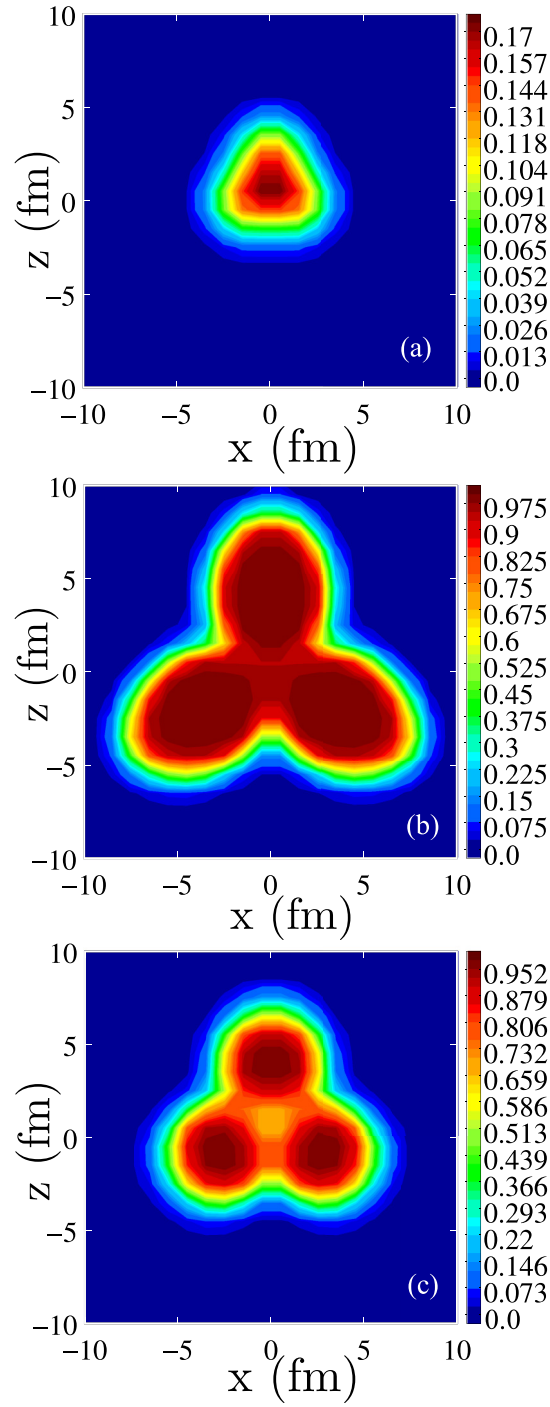

FIG. 2. (a) The total density for the ground state configuration of the three alpha particles plotted in the x-z plane. (b) The $n\uparrow$ localization function before the density constraint. (c) The $n\uparrow$ localization function of the ground state configuration after the density constraint minimization.

close to the value 1.0 indicate the prominent positions of the three α particles. It is clear that the α particles are connected by bond like arms. The localization function for protons and spin-down components essentially show the same structure.

We have previously shown that enforcing the Pauli exclusion principle in density-constraint HF calculations has

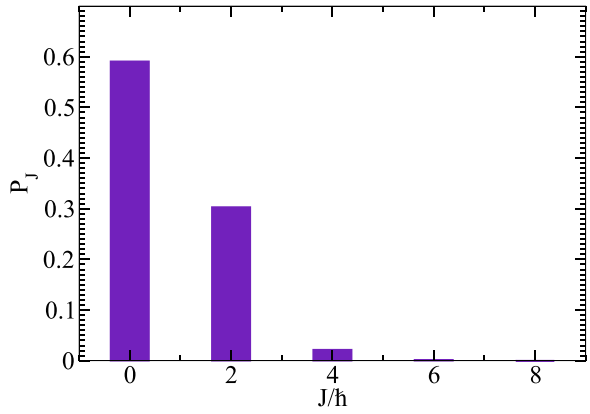

FIG. 3. Angular momentum projection of the ^{12}C ground state configuration.

a strong impact on the spin-orbit energy [51], absorbing a large part of the Pauli repulsion. This is in agreement with the observations that the spin-orbit interaction is the primary driver in partially dissolving the α clusters in the ground state of ^{12}C [16,70,71].

What is also interesting is the evolution of the single-particle parities during the density constrained minimization procedure. Initially, all the α particles are naturally in their s states. While we do not have good parity for the deformed state, at the end of the minimization four of the six neutron or proton single-particle states acquire average negative parity values (not unity), which is appropriate for the ground state of ^{12}C. This has been previously observed in the dynamical collapse of the metastable linear-chain state in TDHF calculations [31]. The conclusion is that within our approach the ground state of ^{12}C is not a pure α condensate but more of a molecular type state formed by the bonding of three αs.

We have performed angular momentum projection of this ground state configuration following the method discussed in Ref. [15], which is shown in Fig. 3. It is interesting to see that the major component is $J = 0$, as one would expect for the ground state. There is, however, a significant $J = 2$ component implying that, in principle, ground state observables (e.g., binding energy) should be evaluated from the $J = 0$ projected state. Note that there is little contribution from $J > 2$.

Using the same procedure we have also tried to identify the configuration that was observed in Ref. [31], which could be the candidate for the Hoyle state at DFT level. It is believed to arise from the bending of the linear-chain three α configuration, which was seen in TDHF calculations of the triple-α reaction [31] as an intermediate state during the dynamical collapse of the linear-chain state to the spherical ground state. There, the dynamical transition of some of the initial single-particle parities from an s state to a p state was also noted. The observed metastable bent-arm configuration occurred during this parity transition. Here, we also looked at the changing parities of the single-particle states as we changed the values of d_2 and z_3. Again, these are not parity projected states so this is simply a signature for changing single-particle symmetries. Dependence on parity was also studied in cluster model calculations [72]. The location of this configuration is shown in Fig. 1 with a "+" sign. As

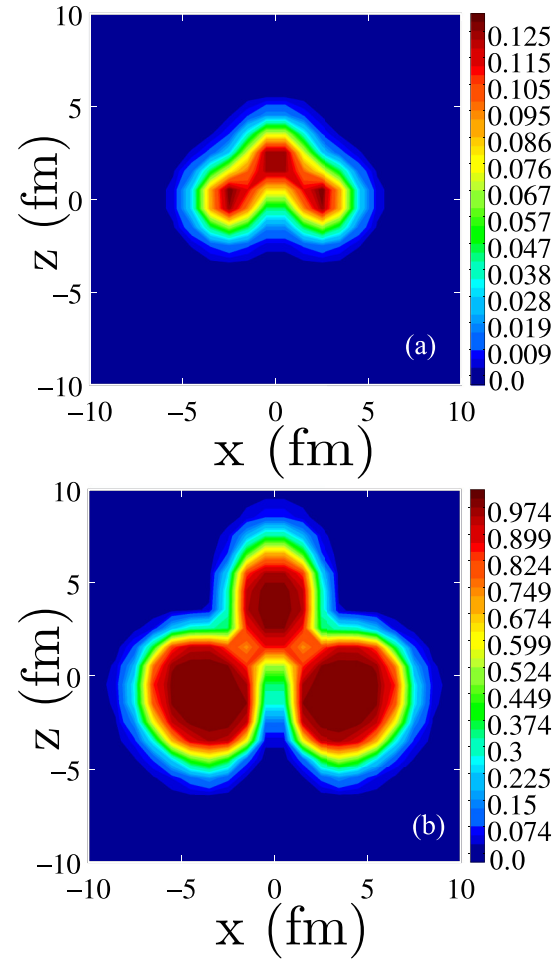

FIG. 4. (a) The total density for the bent-arm state configuration of the three α particles plotted in the x-z plane. (b) The corresponding localization function of the bent-arm state configuration.

we see PES is very soft in the "d2" direction and this point is a very shallow local minimum. It is interesting that the dynamical collapse of the linear chain state also showed that the system spent some time at the bent-arm configuration but there was no discernible minimum in the DC-TDHF potentials (see Fig. 3 of Ref. [31]). This makes the identification of this configuration more tenuous. The lowest energy configuration corresponding to this intermediate state is depicted in Fig. 4 and corresponds to $d_2 = 5.0$ fm and $z_3 = 2.2$ fm. Similar to the ground state case we find this bent-arm mode to be a hybrid configuration of three αs with molecular like bonds between the center alpha particle and the ones on each end, as shown in Fig. 4(a). Unlike the ground state configuration this configuration has only two main bonds and has the shape of an obtuse isosceles triangle. The overlap between the Slater determinant of the ground state configuration and the bent-arm state is on the order of 10^{-3}, which is small enough to consider that these are different eigenstates of the system. The localization function for the bent-arm configuration, shown in Fig. 4(b), is very telling. We see that the two clusters that are on each end are associated with extended $C \approx 1$ regions, indicating that they are closer to becoming pure α particles.

IV. CONCLUSIONS

We have introduced a new framework for studying clusterization in light nuclei, which is based on the constrained density functional theory. The new approach does not make any assumptions about the mathematical form of the single-particle wave functions and employs the full effective interaction. Results show that the ^{12}C ground state is an equilateral triangle, which has a molecular type configuration. The nuclear localization function shows bond like structures being formed among the original alpha particles as a result of antisymmetrization and energy minimization. One can conclude that these configurations are a hybrid between pure mean-field and a pure α particle condensate. From our investigation of the cluster energy surface it is clear that a pure α condensate (characterized by pure s-wave states) would only occur if the three αs are relatively far from each other.

One disadvantage of not using Gaussian type single-particle states or α particles with custom cluster potentials is that we are unable to correct for the spurious center of mass energy. Another is that procedures like angular momentum projection, generator coordinate method, etc., become numerically very challenging for the full effective interaction. This makes detailed spectroscopic comparisons with experiment very difficult. On the other hand one advantage is that this ground state of ^{12}C may be suitable for fusion barrier calculations using frozen Hartree-Fock or density constrained frozen Hartree-Fock methods [51,52], which we plan to investigate in the future. The preparation of the α clustering configuration can also be used for the development and quantification of new energy density functionals, particularly in sectors where the static properties are underinformed by the typical data used in calibration [73,74].

ACKNOWLEDGMENTS

One of the authors (A.S.U.) would like to thank the organizers of the MCD2022 workshop, where some of ideas presented here have been inspired. This work has been supported by the U.S. Department of Energy under award No. DE-SC0013847 (Vanderbilt University), No. DE-SC0013365 (Michigan State University), No. DE-NA0004074 (NNSA, the Stewardship Science Academic Alliances program), and by the Australian Research Council Discovery Project (Project No. DP190100256) funding schemes.

[1] C. A. Barnes, S. Trentalange, and S. C. Wu, in Heavy-Ion Reactions in Nuclear Astrophysics, in *Treatise on Heavy-Ion Science*, edited by D. A. Bromley (Plenum, New York, 1985), Vol. 6, pp. 1–60.

[2] B. M. S. Hansen and J. Liebert, Cool white dwarfs, Annu. Rev. Astron. Astrophys. **41**, 465 (2003).

[3] S. Toonen, G. Nelemans, and S. Portegies Zwart, Supernova Type Ia progenitors from merging double white dwarfs - Using a new population synthesis model, Astron. Astrophys. **546**, A70 (2012).

[4] G. Fruet, S. Courtin, M. Heine, D. G. Jenkins, P. Adsley, A. Brown, R. Canavan, W. N. Catford, E. Charon, D. Curien, S. Della Negra, J. Duprat, F. Hammache, J. Lesrel, G. Lotay, A. Meyer, D. Montanari, L. Morris, M. Moukaddam, J. Nippert, Z. Podolyák *et al.*, Advances in the Direct Study of Carbon Burning in Massive Stars, Phys. Rev. Lett. **124**, 192701 (2020).

[5] K. Mori, M. A. Famiano, T. Kajino, M. Kusakabe, and X. Tang, Impacts of the new carbon fusion cross-sections on type Ia supernovae, Mon. Not. R. Astron. Soc.: Lett. **482**, L70 (2019).

[6] A. Tumino, C. Spitaleri, M. La Cognata, S. Cherubini, G. L. Guardo, M. Gulino, S. Hayakawa, I. Indelicato, L. Lamia, H. Petrascu, R. G. Pizzone, S. M. R. Puglia, G. G. Rapisarda, S. Romano, M. L. Sergi, R. Spartá, and L. Trache, An increase in the ^{12}C + ^{12}C fusion rate from resonances at astrophysical energies, Nature (London) **557**, 687 (2018).

[7] R. L. Cooper, A. W. Steiner, and E. F. Brown, Possible resonances in the ^{12}C + ^{12}C fusion rate and superburst ignition, Astrophys. J. **702**, 660 (2009).

[8] T. Spillane, F. Raiola, C. Rolfs, D. Schürmann, F. Strieder, S. Zeng, H.-W. Becker, C. Bordeanu, L. Gialanella, M. Romano, and J. Schweitzer, ^{12}C + ^{12}C Fusion Reactions near the Gamow Energy, Phys. Rev. Lett. **98**, 122501 (2007).

[9] W. P. Tan, A. Boeltzig, C. Dulal, R. J. deBoer, B. Frentz, S. Henderson, K. B. Howard, R. Kelmar, J. J. Kolata, J. Long, K. T. Macon, S. Moylan, G. F. Peaslee, M. Renaud, C. Seymour, G. Seymour, B. Vande Kolk, M. Wiescher, E. F. Aguilera, P. Amador-Valenzuela *et al.*, New Measurement of ^{12}C + ^{12}C Fusion Reaction at Astrophysical Energies, Phys. Rev. Lett. **124**, 192702 (2020).

[10] E. Monpribat, S. Martinet, S. Courtin, M. Heine, S. Ekström, D. G. Jenkins, A. Choplin, P. Adsley, D. Curien, M. Moukaddam, J. Nippert, S. Tsiatsiou, and G. Meynet, A new ^{12}C + ^{12}C nuclear reaction rate: Impact on stellar evolution, Astron. Astrophys. **660**, A47 (2022).

[11] P. Adsley, M. Heine, D. G. Jenkins, S. Courtin, R. Neveling, J. W. Brümmer, L. M. Donaldson, N. Y. Kheswa, K. C. W. Li, D. J. Marín-Lámbarri, P. Z. Mabika, P. Papka, L. Pellegri, V. Pesudo, B. Rebeiro, F. D. Smit, and W. Yahia-Cherif, Extending the Hoyle-State Paradigm to ^{12}C + ^{12}C Fusion, Phys. Rev. Lett. **129**, 102701 (2022).

[12] M. Freer, H. Horiuchi, Y. Kanada-En'yo, D. Lee, and Ulf-G. Meißner, Microscopic clustering in light nuclei, Rev. Mod. Phys. **90**, 035004 (2018).

[13] P.-G. Reinhard, J. A. Maruhn, A. S. Umar, and V. E. Oberacker, Localization in light nuclei, Phys. Rev. C **83**, 034312 (2011).

[14] J.-P. Ebran, E. Khan, T. Nikšić, and D. Vretenar, How atomic nuclei cluster, Nature (London) **487**, 341 (2012).

[15] S. Shinohara, H. Ohta, T. Nakatsukasa, and K. Yabana, Configuration mixing calculation for complete low-lying spectra with a mean-field Hamiltonian, Phys. Rev. C **74**, 054315 (2006).

[16] Y. Fukuoka, S. Shinohara, Y. Funaki, T. Nakatsukasa, and K. Yabana, Deformation and cluster structures in ^{12}C studied with configuration mixing using Skyrme interactions, Phys. Rev. C **88**, 014321 (2013).

[17] M. Yasue, T. Tanabe, F. Soga, J. Kokame, F. Shimokoshi, J. Kasagi, Y. Toba, Y. Kadota, T. Ohsawa, and K. Furuno, Deformation parameter of ^{12}C via ^{12}C(α, α') and ^{12}C$(\alpha, \alpha'\alpha)$ reactions, Nucl. Phys. A **394**, 29 (1983).

[18] M. Kumar Raju, J. N. Orce, P. Navrátil, G. C. Ball, T. E. Drake, S. Triambak, G. Hackman, C. J. Pearson, K. J. Abrahams, E. H. Akakpo, H. Al Falou, R. Churchman, D. S. Cross, M. K. Djongolov, N. Erasmus, P. Finlay, A. B. Garnsworthy, P. E. Garrett, D. G. Jenkins, R. Kshetri *et al.*, Reorientation-effect measurement of the first 2^+ state in ^{12}C: Confirmation of oblate deformation, Phys. Lett. B **777**, 250 (2018).

[19] D. J. Marín-Lámbarri, R. Bijker, M. Freer, M. Gai, T. Kokalova, D. J. Parker, and C. Wheldon, Evidence for Triangular $\mathcal{D}_{3h}$ Symmetry in ^{12}C, Phys. Rev. Lett. **113**, 012502 (2014).

[20] H. Morinaga, Interpretation of some of the excited states of $4n$ self-conjugate nuclei, Phys. Rev. **101**, 254 (1956).

[21] A. Tohsaki, H. Horiuchi, P. Schuck, and G. Röpke, Alpha Cluster Condensation in ^{12}C and ^{16}O, Phys. Rev. Lett. **87**, 192501 (2001).

[22] T. Ichikawa, J. A. Maruhn, N. Itagaki, and S. Ohkubo, Linear Chain Structure of Four-α Clusters in ^{16}O, Phys. Rev. Lett. **107**, 112501 (2011).

[23] M. Girod and P. Schuck, α-Particle Clustering from Expanding Self-Conjugate Nuclei within the Hartree-Fock-Bogoliubov Approach, Phys. Rev. Lett. **111**, 132503 (2013).

[24] J.-P. Ebran, E. Khan, T. Nikšić, and D. Vretenar, Density functional theory studies of cluster states in nuclei, Phys. Rev. C **90**, 054329 (2014).

[25] Y. Funaki, Hoyle band and α condensation in ^{12}C, Phys. Rev. C **92**, 021302(R) (2015).

[26] P. W. Zhao, N. Itagaki, and J. Meng, Rod-shaped Nuclei at Extreme Spin and Isospin, Phys. Rev. Lett. **115**, 022501 (2015).

[27] J.-P. Ebran, E. Khan, T. Nikšić, and D. Vretenar, Localization and clustering in atomic nuclei, J. Phys. G **44**, 103001 (2017).

[28] P. Marević, J.-P. Ebran, E. Khan, T. Nikšić, and D. Vretenar, Cluster structures in ^{12}C from global energy density functionals, Phys. Rev. C **99**, 034317 (2019).

[29] T. Ichikawa and N. Itagaki, Optimization of basis functions for multiconfiguration mixing using the replica exchange Monte Carlo method and its application to ^{12}C, Phys. Rev. C **105**, 024314 (2022).

[30] K. Wang and B.-N. Lu, The angular momentum and parity projected multidimensionally constrained relativistic Hartree–Bogoliubov model, Comm. Theor. Phys. **74**, 015303 (2022).

[31] A. S. Umar, J. A. Maruhn, N. Itagaki, and V. E. Oberacker, Microscopic Study of the Triple-α Reaction, Phys. Rev. Lett. **104**, 212503 (2010).

[32] P. D. Stevenson and J. L. Willerton, A time-dependent Hartree-Fock study of triple-alpha dynamics, SciPost Phys. Proc. **3**, 047 (2020).

[33] J. Bishop, G. V. Rogachev, S. Ahn, E. Aboud, M. Barbui, A. Bosh, C. Hunt, H. Jayatissa, E. Koshchiy, R. Malecek, S. T. Marley, E. C. Pollacco, C. D. Pruitt, B. T. Roeder, A. Saastamoinen, L. G. Sobotka, and S. Upadhyayula, Almost medium-free measurement of the Hoyle state direct-decay component with a TPC, Phys. Rev. C **102**, 041303(R) (2020).

[34] J. Bishop, C. E. Parker, G. V. Rogachev, S. Ahn, E. Koshchiy, K. Brandenburg, C. R. Brune, R. J. Charity, J. Derkin, N. Dronchi, G. Hamad, Y. Jones-Alberty, T. Kokalova, T. N. Massey, Z. Meisel, E. V. Ohstrom, S. N. Paneru, E. C. Pollacco, M. Saxena, N. Singh, R. Smith, L. G. Sobotka, D. Soltesz, S. K. Subedi, A. V. Voinov, J. Warren, and C. Wheldon, Neutron-upscattering enhancement of the triple-alpha process, Nat. Commun. **13**, 2151 (2022).

[35] E. Epelbaum, H. Krebs, D. Lee, and Ulf-G. Meißner, *Ab Initio* Calculation of the Hoyle State, Phys. Rev. Lett. **106**, 192501 (2011).

[36] E. Epelbaum, H. Krebs, T. A. Lähde, D. Lee, and Ulf-G. Meißner, Structure and Rotations of the Hoyle State, Phys. Rev. Lett. **109**, 252501 (2012).

[37] S. Shen, T. A. Lähde, D. Lee, and U.-G. Meißner, Emergent geometry and duality in the carbon nucleus, Nat. Commun. **14**, 2777 (2023).

[38] D. M. Brink, Many-body description of nuclear structure and reactions, in *Proceedings of the International School of Physics "Enrico Fermi" Course XXXVI* (Academic Press, New York, 1966), p. 247.

[39] Y. Kanada-En'yo, H. Horiuchi, and A. Ono, Structure of Li and Be isotopes studied with antisymmetrized molecular dynamics, Phys. Rev. C **52**, 628 (1995).

[40] Y. Kanada-En'yo, The structure of ground and excited states of ^{12}C, Prog. Theor. Phys. **117**, 655 (2007).

[41] Y. Kanada-En'yo and N. Hinohara, Collective model for cluster motion in ^{8}Be, ^{12}C, and ^{16}O systems based on microscopic 2α, 3α, and 4α models, Phys. Rev. C **106**, 054312 (2022).

[42] T. Neff and H. Feldmeier, Cluster structures within Fermionic molecular dynamics, Nucl. Phys. A **738**, 357 (2004).

[43] W. von Oertzen, Martin Freer, and Yoshiko Kanada–En'yo, Nuclear clusters and nuclear molecules, Phys. Rep. **432**, 43 (2006).

[44] Y. Funaki, T. Yamada, H. Horiuchi, G. Röpke, P. Schuck, and A. Tohsaki, α-Particle Condensation in ^{16}O Studied with a Full Four-Body Orthogonality Condition Model Calculation, Phys. Rev. Lett. **101**, 082502 (2008).

[45] M. Freer, The clustered nucleus–cluster structures in stable and unstable nuclei, Rep. Prog. Phys. **70**, 2149 (2007).

[46] Y. Yuta and K.-E. Yoshiko, 3α cluster structure and monopole transition in ^{12}C and ^{14}C, Prog. Theor. Exp. Phys. **2016**, 123D04 (2016).

[47] A. Tohsaki, H. Horiuchi, P. Schuck, and G. Röpke, Colloquium: Status of α-particle condensate structure of the Hoyle state, Rev. Mod. Phys. **89**, 011002 (2017).

[48] R. Y. Cusson, P.-G. Reinhard, M. R. Strayer, J. A. Maruhn, and W. Greiner, Density as a constraint and the separation of internal excitation energy in TDHF, Z. Phys. A **320**, 475 (1985).

[49] A. S. Umar, M. R. Strayer, R. Y. Cusson, P.-G. Reinhard, and D. A. Bromley, Time-dependent Hartree-Fock calculations of ^{4}He + ^{14}C, ^{12}C + ^{12}C (0^+), and ^{4}He + ^{20}Ne molecular formations, Phys. Rev. C **32**, 172 (1985).

[50] C. Simenel and A. S. Umar, Heavy-ion collisions and fission dynamics with the time–dependent Hartree-Fock theory and its extensions, Prog. Part. Nucl. Phys. **103**, 19 (2018).

[51] C. Simenel, A. S. Umar, K. Godbey, M. Dasgupta, and D. J. Hinde, How the Pauli exclusion principle affects fusion of atomic nuclei, Phys. Rev. C **95**, 031601(R) (2017).

[52] A. S. Umar, C. Simenel, and K. Godbey, Pauli energy contribution to the nucleus-nucleus interaction, Phys. Rev. C **104**, 034619 (2021).

[53] A. S. Umar and V. E. Oberacker, Center-of-mass motion and cross-channel coupling in the time-dependent Hartree-Fock theory, J. Phys. G: Nucl. Part. Phys. **36**, 025101 (2009).
[54] A. D. Becke and K. E. Edgecombe, A simple measure of electron localization in atomic and molecular systems, J. Chem. Phys. **92**, 5397 (1990).
[55] T. Li, M. Z. Chen, C. L. Zhang, W. Nazarewicz, and M. Kortelainen, Nucleon localization function in rotating nuclei, Phys. Rev. C **102**, 044305 (2020).
[56] E. Khan, L. Heitz, F. Mercier, and J.-P. Ebran, α-particle formation and clustering in nuclei, Phys. Rev. C **106**, 064330 (2022).
[57] Y. M. Engel, D. M. Brink, K. Goeke, S. J. Krieger, and D. Vautherin, Time-dependent Hartree-Fock theory with Skyrme's interaction, Nucl. Phys. A **249**, 215 (1975).
[58] M. Bender, P.-H. Heenen, and P.-G. Reinhard, Self-consistent mean-field models for nuclear structure, Rev. Mod. Phys. **75**, 121 (2003).
[59] E. Perlińska, S. G. Rohoziński, J. Dobaczewski, and W. Nazarewicz, Local density approximation for proton-neutron pairing correlations: Formalism, Phys. Rev. C **69**, 014316 (2004).
[60] M. Matsumoto and Y. Tanimura, Visualization of nuclear many-body correlations with the most probable configuration of nucleons, Phys. Rev. C **106**, 014307 (2022).
[61] A. S. Umar and V. E. Oberacker, Three-dimensional unrestricted time-dependent Hartree-Fock fusion calculations using the full Skyrme interaction, Phys. Rev. C **73**, 054607 (2006).
[62] Ka–Hae Kim, T. Otsuka, and P. Bonche, Three-dimensional TDHF calculations for reactions of unstable nuclei, J. Phys. G: Nucl. Part. Phys. **23**, 1267 (1997).
[63] C. Simenel, Nuclear quantum many-body dynamics, Eur. Phys. J. A **48**, 152 (2012).
[64] C. Bottcher, M. R. Strayer, A. S. Umar, and P.-G. Reinhard, Damped relaxation techniques to calculate relativistic bound-states, Phys. Rev. A **40**, 4182 (1989).
[65] A. S. Umar, M. R. Strayer, J. S. Wu, D. J. Dean, and M. C. Güçlü, Nuclear Hartree-Fock calculations with splines, Phys. Rev. C **44**, 2512 (1991).
[66] A. S. Umar, J. Wu, M. R. Strayer, and C. Bottcher, Basis-spline collocation method for the lattice solution of boundary-value-problems, J. Comput. Phys. **93**, 426 (1991).
[67] I. Tanihata, H. Hamagaki, O. Hashimoto, Y. Shida, N. Yoshikawa, K. Sugimoto, O. Yamakawa, T. Kobayashi, and N. Takahashi, Measurements of Interaction Cross Sections and Nuclear Radii in the Light *p*-Shell Region, Phys. Rev. Lett. **55**, 2676 (1985).
[68] I. Angeli and K. P. Marinova, Table of experimental nuclear ground state charge radii: An update, At. Data Nucl. Data Tables **99**, 69 (2013).
[69] J. H. Kelley, J. E. Purcell, and C. G. Sheu, Energy levels of light nuclei A = 12, Nucl. Phys. A **968**, 71 (2017).
[70] N. Itagaki, S. Aoyama, S. Okabe, and K. Ikeda, Cluster-shell competition in light nuclei, Phys. Rev. C **70**, 054307 (2004).
[71] W. Horiuchi and N. Itagaki, Imprints of α clustering in the density profiles of ^{12}C and ^{16}O, Phys. Rev. C **107**, L021304 (2023).
[72] N. Itagaki, W. von Oertzen, and S. Okabe, Linear-chain structure of three alpha clusters in ^{13}C, Phys. Rev. C **74**, 067304 (2006).
[73] J. D. McDonnell, N. Schunck, D. Higdon, J. Sarich, S. M. Wild, and W. Nazarewicz, Uncertainty Quantification for Nuclear Density Functional Theory and Information Content of New Measurements, Phys. Rev. Lett. **114**, 122501 (2015).
[74] K. Godbey, A. S. Umar, and C. Simenel, Theoretical uncertainty quantification for heavy-ion fusion, Phys. Rev. C **106**, L051602 (2022).